A R C H I V E S O F M E T A L L U R G Y A N D M A T E R I A L S
Volume 55 2010 Issue 3

J. RYŚ*, M. WITKOWSKA*

INFLUENCE OF BAND-LIKE MORPHOLOGY ON MICROSTRUCTURE AND TEXTURE EVOLUTION IN ROLLED SUPER-DUPLEX STEEL

WPŁYW PASMOWEJ MORFOLOGII NA ROZWÓJ MIKROSTRUKTURY I TEKSTURY W WALCOWANEJ STALI TYPU SUPER-DUPLEX

The present investigations concern the formation of rolling textures and the evolution of ferrite and austenite microstructures in cold-rolled sheets of super-duplex stainless steel UR52N+. The preliminary thermo-mechanical treatment included hot-rolling with subsequent solution annealing at the temperatures 1150°C and 1050°C. Afterwards the steel plates were subjected to cold-rolling over a wide range of reductions parallel to the direction of hot-deformation.

The band-like morphology of the ferrite-austenite structure formed upon hot- and subsequent cold-rolling creates different conditions for plastic deformation in comparison to one-phase steels. Nevertheless basic mechanisms controlling the deformation behavior and the formation of ferrite and austenite rolling textures in the examined super-duplex steel are essentially the same as in single phase steels. Microstructure development in the ferrite and austenite bands results first of all from the following factors; crystallographic structure, chemical composition, stacking fault energy and orientation distribution, and only to some extent from phase interaction. A characteristic feature is the rolling texture formation within the bands of both phases, which show stability over a wide range of deformations. The dominating texture components, i.e. the orientations {001}<110> in ferrite and {110}<112> in austenite, are typical orientations for one-phase steels.

Keywords: super-duplex stainless steel, cold-rolling, band-like morphology, deformation mechanisms, ferrite and austenite rolling textures

Prezentowane badania dotyczą tworzenia się tekstur walcowania oraz rozwoju mikrostruktur ferrytu i austenitu w walcowanych na zimno blachach z nierdzewnej stali w gatunku UR52N+ typu super-duplex. Wstępna obróbka cieplno-mechaniczna obejmowała walcowanie na gorąco oraz przesycanie z temperatur 1150°C oraz 1050°C. Stal poddano następnie walcowaniu na zimno w szerokim zakresie odkształceń równolegle do kierunku przeróbki plastycznej na gorąco.

Pasmowa morfologia struktury ferrytu i austenitu tworząca się podczas walcowania na gorąco a następnie na zimno stwarza odmienne warunki dla przebiegu odkształcenia plastycznego w porównaniu do stali jednofazowych. Niemniej podstawowe mechanizmy kontrolujące sposób odkształcenia oraz tworzenie się tekstur walcowania obu składowych faz w badanej stali super-duplex są zasadniczo takie same jak w przypadku stali jednofazowych. Rozwój mikrostruktury w pasmach ferrytu i austenitu wynika przede wszystkim z następujących czynników; budowy krystalograficznej, składu chemicznego, energii błędu ułożenia i rozkładu orientacji, a tylko w pewnej mierze z oddziaływania obu faz. Charakterystyczny jest przebieg tworzenia się tekstur walcowania w pasmach obu faz, które wykazują stabilność w szerokim zakresie odkształceń. Dominujące składowe tekstury, tzn. orientacje {001}<110> w ferrycie i {110}<112>, w austenicie, są typowymi orientacjami w stalach jednofazowych.

1. Introduction

Plastic deformation is one of the essential technological steps for a major part of products manufactured of duplex stainless steels. Processes of hot-working are usually followed by annealing treatment conducted within an appropriate temperature range and one of the final operations is cold-deformation [1,2]. In the course of hot- and subsequent cold-rolling duplex type steels develop band-like ferrite-austenite morphology. This specific two-phase structure creates different conditions for plastic deformation in comparison to single phase steels. It is considered that the interaction of both constituent phases upon deformation exerts fairly significant influence on microstructure and texture evolution in ferrite and austenite bands and in consequence affects the material properties and its behavior upon further processing [3].

* DEPARTMENT OF PHYSICAL AND POWDER METALLURGY, AGH-UNIVERSITY OF SCIENCE AND TECHNOLOGY, 30-059 KRAKÓW, 30 MICKIEWICZA AV., POLAND

Both constituent phases are plastically deformed upon hot- and cold-rolling. Formation and subsequent reduction in thickness of the ferrite and austenite bands result in so-called "pancake" structure. As a consequence the (α/γ) phase interfaces, which are strong obstacles for dislocation motion, are arranged mostly parallel to the rolling plane. That is why conditions for development of ferrite and austenite microstructures and formation of rolling textures in both constituent phases should changed in comparison to single phase steels [4÷7].

From a number of investigations it results that the anisotropy in mechanical properties of duplex steel sheets is not only the effect of a specific morphology of the (α/γ) two-phase structure but also depends on the crystallographic textures of ferrite and austenite [1,8]. The occurrence of strong initial textures after a preliminary treatment and the specific crystallographic orientation relations between both phases may additionally affect their deformation behaviour in the course of cold-rolling. Plastically compatible deformation of ferrite and austenite bands may result in texture stability over a considerable deformation range changing a character of the final rolling textures [6]. That is why the specific band-like morphology and the starting orientation distributions of the component phases after thermo-mechanical pre-treatment become important factors, which should be taken into account when analysing texture formation of cold-rolled duplex type steels [1,2].

The aim of the present research was to examine rolling texture formation and a development of ferrite and austenite microstructures in a cold-rolled sheet of super-duplex stainless steel UR52N+. Cold-rolling deformation was conducted after the preliminary thermo-mechanical treatment within a wide range of reductions parallel to the hot-rolling direction. The band-like morphology of the constituent phases, major texture components dominating in both phases and the alloying addition of nitrogen were taken into account. The rolling textures of both constituent phases were compared with those in single phase ferritic and austenitic steels [9,10].

2. Material and experimental procedure

The material under examination was the nitrogen alloyed ferritic-austenitic stainless steel of duplex type X3CrNiMoCuN25-6-4. The chemical composition of the steel (Table I), corresponds to the grade UR52N+ (UNS S32520), that is a super-duplex type of stainless steel. These high-alloy steels have the higher contents of alloying elements stabilizing ferrite, i.e. chromium and molybdenum, hence the increased additions of austenite stabilizers; like nitrogen, nickel and copper, to equalize the proportions of ferrite and austenite [11]. On the basis of the chemical composition the value of PREN (Pitting Resistance Equivalent Number) was estimated at about 41, according to the formula PREN = %Cr + 3,3 (%Mo) + 16 (%N) [11];

TABLE I
Chemical composition of the examined super-duplex stainless steel (wt. %)

C	Cr	Ni	Mo	N	Cu	W	Mn
0.03	25.12	5.82	3.59	0.26	1.49	0.023	0.87
Si	Al	Co	Nb	V	P	S	PREN
0.27	0.13	0.068	0.017	0.096	0.018	0.001	41

The material was received in the form of industrially hot-rolled plate with the final thickness h_0 = 13.5 mm. The flat bars cut of the plate were annealed at the temperatures 1150°C and 1050°C for 3 hours with subsequent water quenching and then subjected to reversed rolling at room temperature in laboratory conditions (roll diameter Φ = 160 mm) up to 85% of reduction ($\varepsilon_t \approx 2$). Cold-rolling was conducted parallel to the direction of hot deformation, i.e. $RD_C \| RD_H$ (Fig. 2a). The applied rolling schedule ensured the least strain gradient throughout the cross section in each roll-pass, with the ratio $(L_c/h_m)>1.0$; where $L_c = \sqrt{R\Delta h}$ – the length of the arc of contact, R – radius of rolls, Δh – thickness reduction per pass and h_m – the mean thickness of the sheet. It is assumed that for such a rolling schedule the compressive strain penetrates throughout the whole thickness of the sheet in each roll-pass and a deformation rate of the centre layer, parallel to the rolling plane, is close to that of the subsurface layers [5,12].

Metallographic analysis of the ferrite-austenite initial morphology after hot-rolling and solution treatment (Figs. 1a-c) and observations of the (α/γ) band-like structure formed in the course of cold-rolling (Figs. 3b,c) were carried out by means of optical microscopy (Neophot-2 and Axiovert-200 MAT). The analysis of deformation mechanisms within the bands of both phases based on microstructures examined on longitudinal sections (ND_C-RD_C) of cold-rolled sheets (Figs. 9÷13) and obtained by means of transmission electron microscopy (Philips CM-20 and Tecnai G2 F20).

X-ray investigations were conducted by means of Bruker diffractometer D8 Advance, using Co Kα radiation ($\lambda_{K\alpha}$ = 0.179 nm). X-ray examination included texture measurements and phase analysis from the centre layers of the rolled sheets, for the initial state and after selected rolling reduc-

tions (Figs. 2, 4). Texture analysis was based on the orientation distribution functions (ODFs) calculated from experimental (incomplete) pole figures recorded of three planes for each of the constituent phases, i.e. the {110}, {100} and {211} planes for the bcc α-phase and the {111}, {100} and {110} planes for the fcc γ-phase. The values of the orientation distribution functions f(g) were examined along the typical orientation fibres; α_1=<110> || RD, γ=<111> || ND, ε=<001> || ND for ferrite and α=<110> || ND, η=<001> || RD, τ=<110> || TD for austenite (Figs. 5, 6).

3. Results and discussion

3.1. Initial morphology and starting textures

The morphology of the (α/γ) two-phase structure and the phase composition of a definite ferritic-austenitic stainless steel depend on a type of applied hot-deformation process and conditions of subsequent solution treatment. Detailed metallographic analysis concerning the ferrite-austenite morphology and the volume fractions of both constituent phases after the preliminary thermo-mechanical treatment in the UR52N+ grade of super-duplex stainless steel is given by the present authors elsewhere [13].

The ferrite-austenite morphology in examined duplex steel after hot-rolling and subsequent solution treatment at the temperatures 1150°C and 1050°C, is shown in Figures 1a÷c. After hot-rolling the volume fraction of austenite (V_V^A) was estimated at about 39% and the ferrite-austenite structure displayed certain degree of heterogeneity. On the longitudinal section (ND_H-RD_H) of the hot-rolled plate the areas with strongly pronounced banding predominated. Nearly continuous and elongated parallel to RD_H bands of austenite, with differentiated thickness were observed within the ferrite matrix (V_V^F >60%) [13]. After solution annealing at the temperature 1150°C the volume fractions of ferrite and austenite changed only by a few percent, V_V^A ~42% and V_V^F ~58% respectively. Thus the ferritic α-phase was still more continuous and constituted the matrix with bands or elongated islands of the austenitic γ-phase. On the other hand after annealing at the temperature 1050°C the volume fractions of both phases were equalized (V_V^F = V_V^A ~50%) and the phase composition exhibited exactly a duplex character. Pronounced directionality of the ferrite-austenite structure observed in hot-rolled plate on the longitudinal (ND_H-RD_H) section (Fig. 1a) remained essentially unchanged after the solution treatment and the regions with considerable degree of banding still predominated (Figs. 1b,c). It should be noted however, that the areas of the γ-phase arranged and elongated parallel to the direction of hot-rolling RD_H were less continuous, especially after the solution annealing at 1150°C, that is for smaller volume fraction of austenite (V_V^A ~42%) [13].

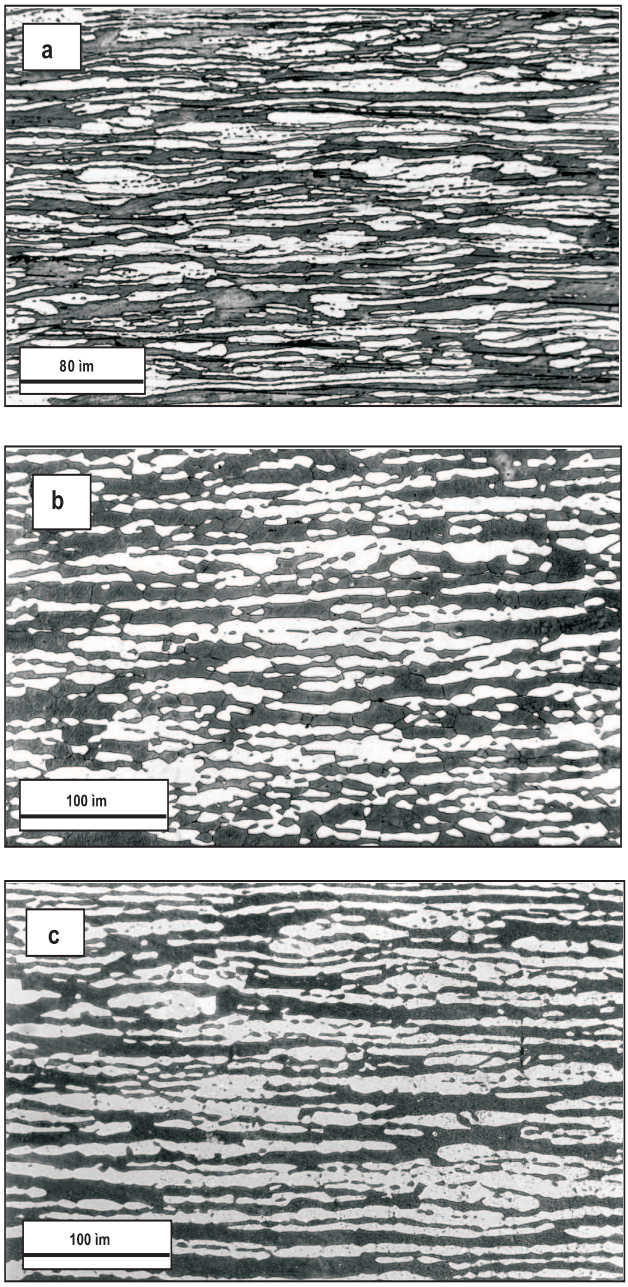

Fig. 1. The ferrite-austenite morphology after hot-rolling (a) and subsequent solution treatment at the temperatures 1150°C (b) and 1050°C (c) on the longitudinal section (ND_H-RD_H) of the plate

Texture measurements conducted after hot-rolling revealed noticeably stronger texture of ferrite (Fig. 2a,b). The austenitic γ-phase exhibited sharp but relatively week cubic texture with the maximum intensity f(g)=3.9. The strongest component,

i.e. the {100}<001> orientation, was detected on the background of nearly random texture with minor components close to alloy type texture {110}<112> (Fig. 2a). The dominating cube component revealed within the austenite texture is usually attributed to dynamic or static recrystallization which proceeded in the course of hot-rolling [1,2]. The major texture component in the ferritic α-phase was the {001}<110> rotated cubic orientation from the inhomogeneous fibers α_1=<110> || RD and ε =<001> || ND, with the maximum intensity f(g)=10.9 (Fig. 2b.). Such a orientation distribution, close to the cold-rolling texture of ferrite, indicates that dynamic recovery occurred the predominant process in the course of hot-rolling instead of recrystallization [1,2].

After solution treatment at the temperatures 1150°C (ST1) and 1050°C (ST2) the dominating orientations from the hot-rolling texture remained the major texture components in both constituent phases (Fig. 2a,b). In the case of the austenitic γ-phase changes in a texture character after annealing at both temperatures occurred relatively small. The austenite annealing texture remained weak with the strongest {100}<001> cubic component having the intensities f(g)=4.4 and f(g)=2.8 respectively. Additionally at the temperature 1150°C the orientations close to {110}<111> appeared in the austenite texture and at the temperature 1050°C weak η-fiber including the {110}<001> Goss orientation (Fig. 2a).

The major component of the ferrite texture after hot-rolling, i.e. the {001}<110> rotated cubic orientation, remained the dominant texture component after solution annealing at 1150°C and 1050°C, however strong fluctuations of texture intensity were detected for both temperatures (Fig. 2b). After solution treatment at 1150°C the {001}<110> orientation from the limited ε- and α_1-fibers was definitely the strongest texture component and showed the intensity f(g)=15.2 (Fig. 2b). For the annealing temperature 1050°C the ferrite texture occurred relatively weak and may be described by the inhomogeneous ε-fiber and the limited α_1-fiber. The strongest component remained the {001}<110> rotated cubic orientation with the intensity f(g)=3.6. Additionally the {100}<001> cubic component appeared within the ferrite annealing texture (Fig. 2b).

Differences in the intensity of the ferrite annealing textures and some changes of the orientation distribution may be in part attributed to the processes taking place within that temperature range, i.e. the ($\gamma \leftrightarrow \alpha$) phase transformation and recrystallization of the ferritic α-phase, however a very important factor is the specific character of two-phase structure.

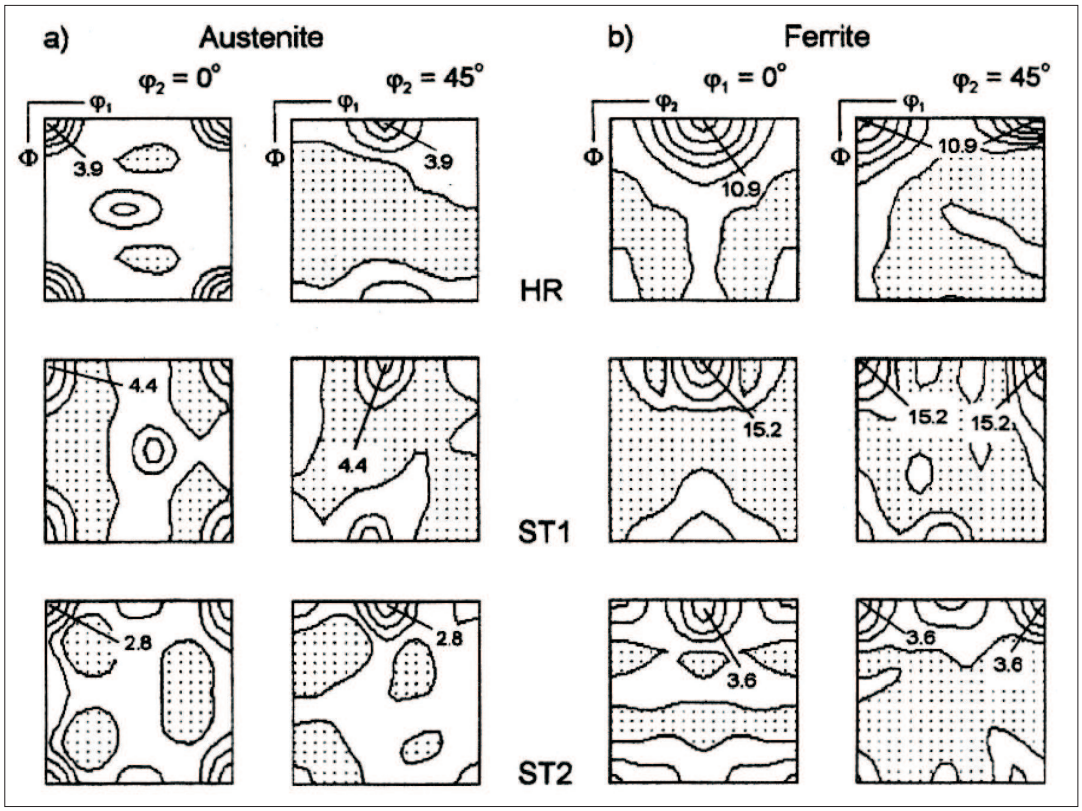

Fig. 2. Orientation distribution functions (ODFs) in sections φ_2 = 0° and φ_2 = 45° for austenite (a); φ_1 = 0° and φ_2 = 45° for ferrite (b), after hot-rolling (HR) and after the solution treatment at 1150°C (ST1) and 1050°C (ST2), from the centre layer of the plate

Taking into account the inhomogeneous distribution of thick ferrite and austenite bands after the thermo-mechanical pre-treatment and the penetration depth of X-ray radiation, the relative texture intensities of both constituent phases should be interpreted qualitatively at the early stages of processing. Nevertheless it should be noted that X-ray measurements reflect the character of the ferrite and austenite textures irrespective of a distribution of the bands of both phases in a given section of the steel plate.

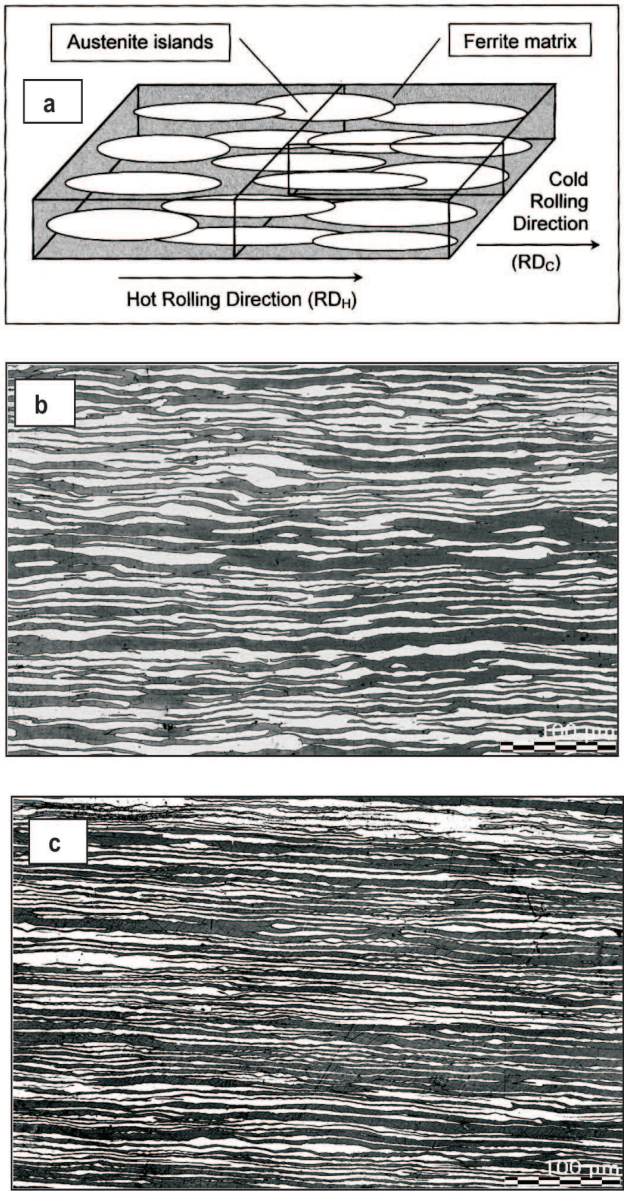

Fig. 3. Schematic illustration of the hot- and cold-rolling procedure (a), band-like morphology of the ferrite-austenite microstructure after 70% (b) and 85% (c) of cold-rolling reduction on the longitudinal section (ND_C-RD_C) of the sheet

3.2. Texture and microstructure after cold-rolling

Cold-rolling deformation was carried out after the preliminary thermo-mechanical treatment within a wide range of reductions parallel to the hot-rolling direction. Schematic illustration of the applied deformation procedure is shown in Figure 3a. In the course of cold-rolling the constituent α- and γ- phases were plastically deformed and formed a specific band-like structure (so-called pancake structure) consisting of alternate ferrite and austenite bands arranged and elongated parallel to the rolling plane. With increasing deformation degree a significant refinement of the microstructure was observed and the thickness of a number of austenite and ferrite bands was reduced to about one micrometer after 85% of deformation. For the case of solution treatment conducted at higher temperature (i.e. 1150°C) the bands of ferrite were thicker and its areas exhibited more continuous character due to the phase composition of the steel [13]. The morphology of the ferrite-austenite microstructure on the longitudinal section (ND_C-RD_C) of the sheet after 70% and 85% of cold-rolling reduction is shown in Figures 3b,c for the annealing temperature 1050°C.

Depending on the applied temperature of solution treatment the UR52N+ duplex steel exhibited significant differences in phase composition as well as some changes in orientation distribution prior to further cold-rolling. Formation of the ferrite and austenite rolling textures after solution annealing at the temperature 1150°C, i.e. for the case the ferritic α-phase constituted the matrix with the volume fraction V_V^F ~60%, was presented elsewhere [7]. The present examination concerns a development of cold-rolling textures after solution annealing at 1050°C, i.e. for the case of phase fraction of 50% for both constituent phases.

3.2.1. Rolling texure formation

In the course of cold-rolling the alloy type texture was formed in austenite already after 30% reduction with the strongest component close to the {110}<112> orientation and the maximum texture intensity f(g)=7.1 (Fig. 4a). At small strains the austenite rolling texture may be described by the limited ($0° < \varphi_1 < 70°$) and inhomogeneous α =<110> || ND fiber and the relatively weak η =<001> || RD fiber with the pronounced {110}<001> orientation. With increasing deformation degree the austenite texture occurred essentially stable up to about 85% of rolling reduction. Within a wide range of deformations the only changes in the rolling texture of austenite concerned the maximum texture intensity, f(g)=7.1÷9.6, and small fluctuations in orientation density observed for minor components from the α- and η- orientation fibers (Figs. 4a, 5). After 85% reduction the character of the austenite rolling texture remained essentially unchanged with the strongest component from the orientation

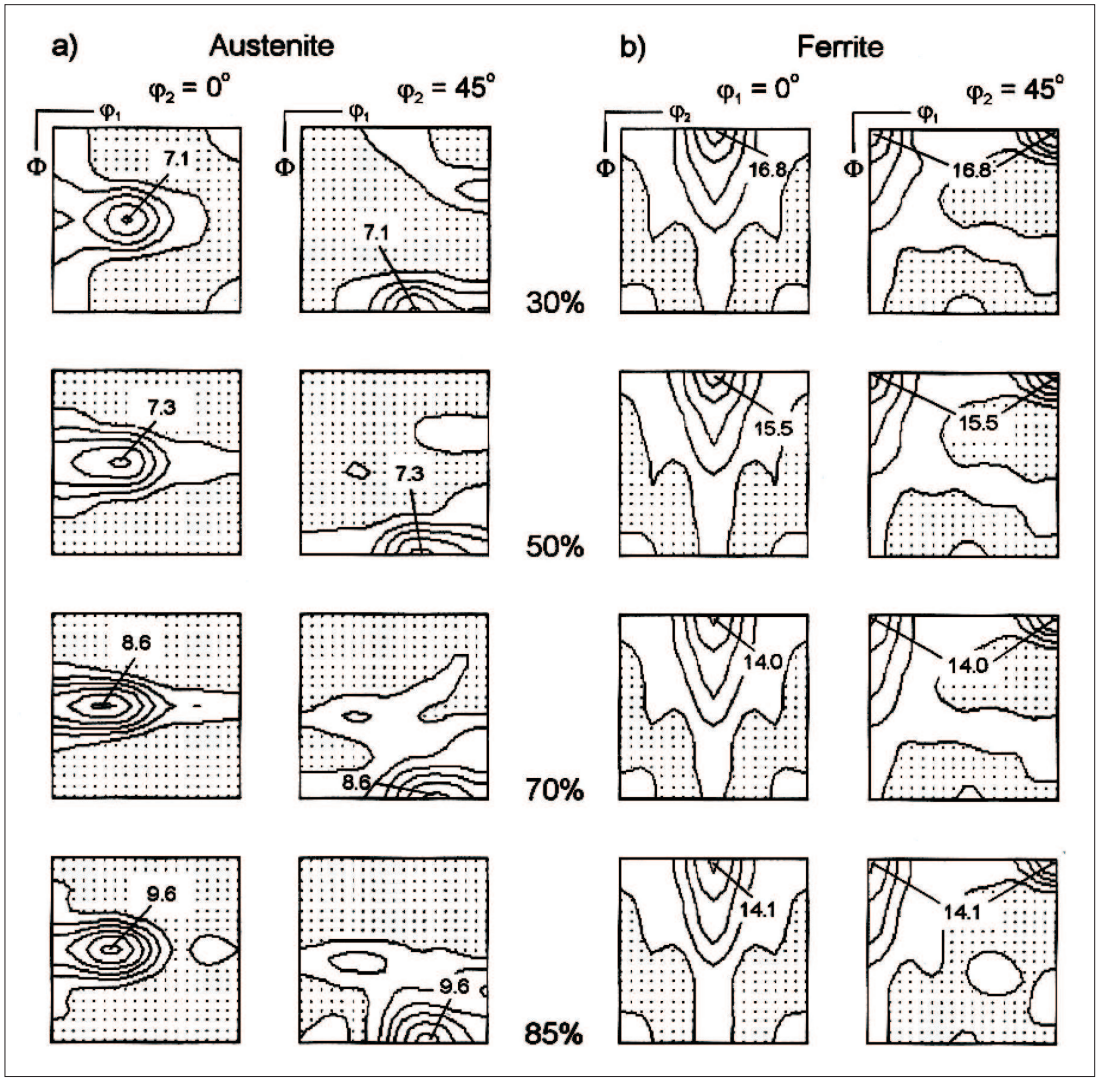

Fig. 4. Orientation distribution functions (ODFs) after selected cold-rolling reductions in sections $\varphi_2 = 0°$ and $\varphi_2 = 45°$ for austenite (a); $\varphi_1 = 0°$ and $\varphi_2 = 45°$ for ferrite (b), from the centre layer of the sheet

range {110}<113÷112> and the texture maximum f(g)=9.6. The rolling texture of austenite at high strains describe the same orientation fibers, i.e. the inhomogeneous α =<110> || ND fiber and the limited and weak η =<001> || ND fiber (Fig. 4a). Formation of the rolling texture very close to alloy type texture {110}<112> starting from early stages of deformation may be explained by low stacking fault energy (SFE) of the austenitic γ-phase. Taking into account the 0.26% addition of nitrogen and the volume fraction of austenite V_V^A =50% after thermo-mechanical treatment, concentration of nitrogen within the γ-phase may be estimated at about 0.5%N. Such a high contents of nitrogen usually results in a considerable decrease of the SFE value of austenite [3,4,14]. Small SFE value of the γ-phase in the examined super-duplex steel determined the deformation behavior and in consequence the texture formation in austenite.

Within a whole range of the applied rolling reductions the texture of ferrite may be essentially described by the inhomogeneous α_1 =<110> || RD and ε =<001> || ND fibers. The ferrite texture was relatively sharp with the strongest {001}<110> rotated cubic component from both orientation fibers, showing intensities from the range f(g)=14.1÷16.8 (Figs. 4b, 6). Stability of the ferrite rolling texture observed after the successive reductions up to 85% of deformation concerned not only the major component {001}<110> but also texture spread with minor texture components. Worthy of notice is the fact that the rotated cubic orientation appeared the dominant component of the ferrite texture for the whole process, including thermo-mechanical treatment and further cold-rolling. An important difference between the rolling textures of the ferritic α-phase in examined duplex steel and those in one-phase ferritic steels is very week γ =<111> || ND fiber, which is nearly absent within a whole deformation range. Only minor components were detected along that fiber, e.g. the {111}<011> orientation (Figs. 4b, 6).

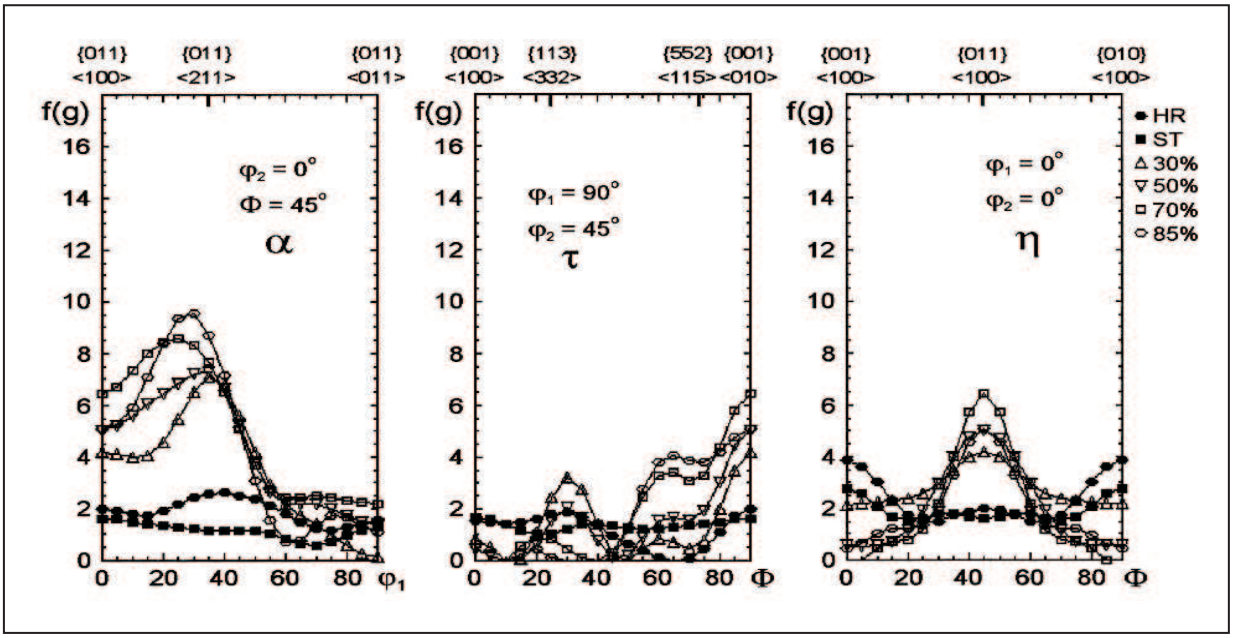

Fig. 5. Values of the orientation distribution functions f(g) for austenite along the orientation fibers; α =<110> || ND, τ =<110> || TD, η =<001> || RD

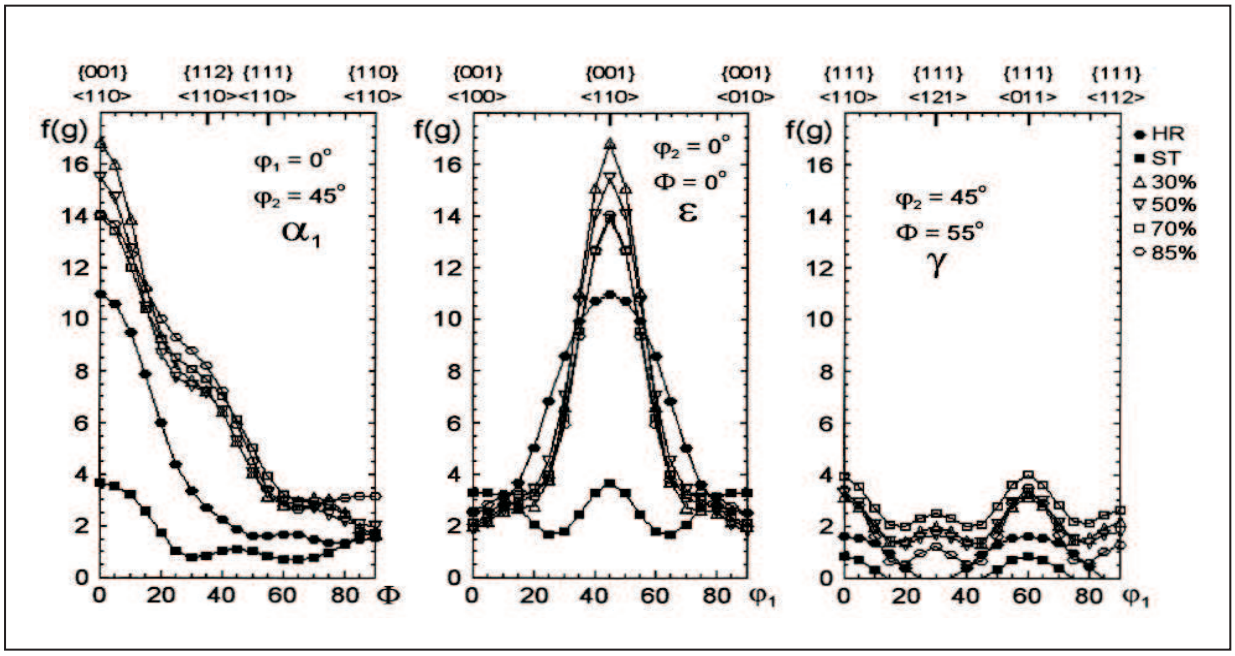

Fig. 6. Values of the orientation distribution functions f(g) for ferrite along the orientation fibers; α_1 =<110> || RD, ε =<001> || ND, γ =<111> || ND

Comparison of the austenite and ferrite rolling textures after solution treatment at the temperature 1150°C (see ref. [7]) and the temperature 1050°C does not reveal any substantial qualitative changes in a texture character. It means that the differences in phase composition, i.e. V_V^F ~60%, V_V^A ~40% at the temperature 1150°C and $V_V^F = V_V^A$ ~50% at 1050°C, do not significantly affect the texture evolution of both constituent phases. Texture stability observed in both phases in the course of cold-rolling is apparently the result of two-phase morphology formed already upon hot-deformation. Domination of the major texture components within ferrite and austenite bands over a wide range of reductions is clearly reflected on the selected ODFs sections (Figs. 4a,b) as well as on the plots of f(g) values along the typical orientation fibers (Figs.5, 6). In general the texture analysis indicates at partially fibrous character and relatively sharp rolling textures of both constituent phases.

3.2.2. Austenite and ferrite microstructures

Analysis of the ferrite and austenite textures developed upon cold-rolling indicates at the texture stability in both phases over a wide deformation range, starting from 30% reduction to about 85% of deformation. The rolling textures of ferrite and austenite were relatively sharp with dominant and strong texture components, namely; the {110}<112> alloy type orientation in austenite and the {001}<110> rotated cubic orientation in ferrite. That is why calculations of the relative shear stresses, i.e. the ratios m = τ/σ, were carried out for the strongest texture components in both phases to establish the most stressed slip (or twin) systems and to explain a deformation behavior within the strongly textured ferrite-austenite banded structure. Schematic illustrations of the potential slip (or twin) systems in both constituent γ- and α- phases in the form of stereographic projections are shown in Figures 7a,b and 8a,b respectively.

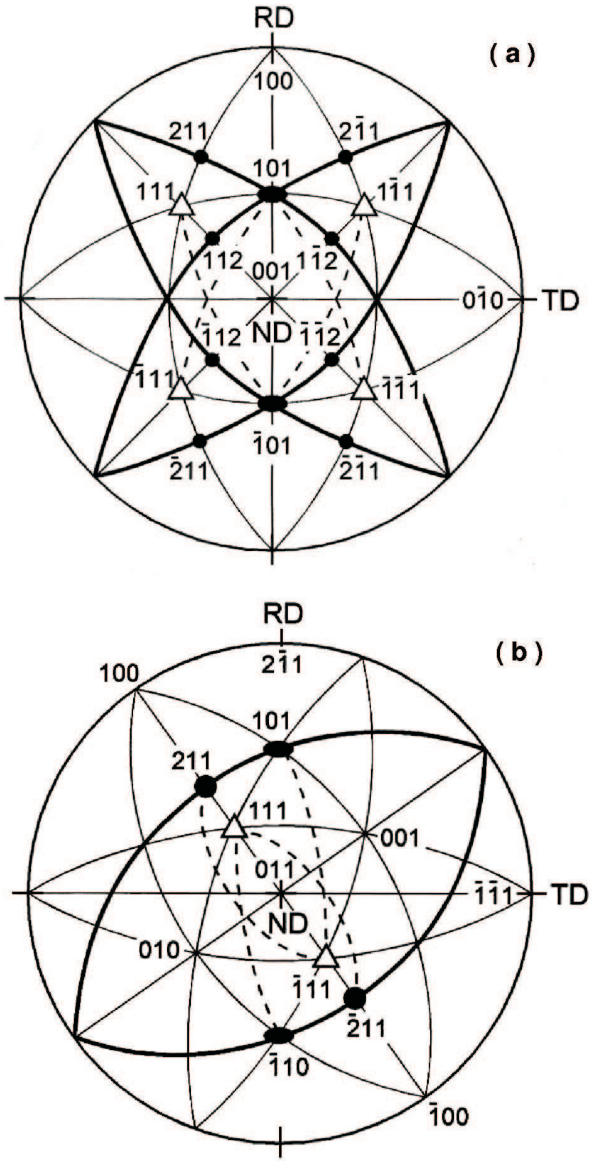

Fig. 7. Stereographic projections showing the most stressed deformation systems for the major texture components in austenite; the {100}<001> orientation after solution treatment (a) and the {110}<112> orientation after cold-rolling (b)

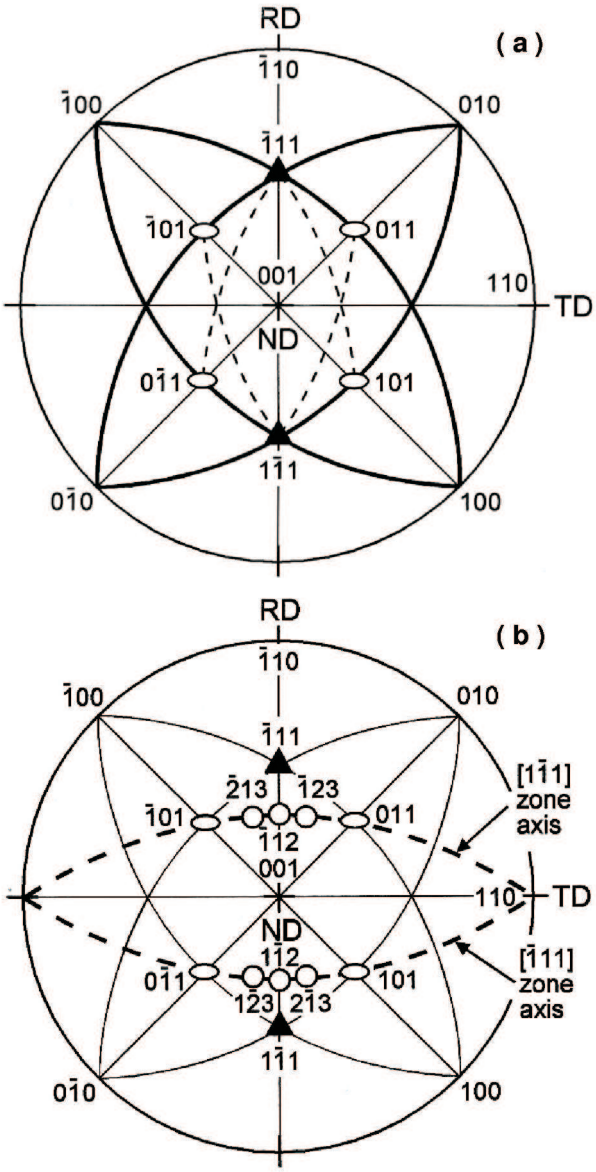

Fig. 8. Stereographic projections showing the most stressed slip systems for the dominant texture component {001}<110> in ferrite; the {110}<111> systems (a) and all slip systems from the [1$\bar{1}$1] and [$\bar{1}$11] zone axes (b)

The strongest component of the austenite texture after solution annealing at 1050°C was the {100}<001> cubic orientation. The highest values of relative shear stresses m=0.816 for that orientation were found in four slip systems {111}<110>. Simultaneously the eight twin systems showed noticeably

lower shear stresses with value of m=0.707 (Fig. 7a). On the other hand for the major component of the austenite rolling texture, i.e. the {110}<112> orientation dominating from about 30% of reduction, the highest values of relative shear stresses (m = 0,816) were in two {111}<110> slip systems, namely the $(\bar{1}11)[101]$ and $(111)[\bar{1}10]$ (Fig. 7b). Additionally, for the two {111}<112> twin systems from the same planes, i.e. $(\bar{1}11)[211]$ and $(111)[\bar{2}11]$, the values of m = 0,786 were only slightly smaller. Hence the deformation of the austenitic γ-phase could proceed in two $(\bar{1}11)$ and (111) slip planes, which were symmetrical with respect to RD (Fig. 7b).

Microstructure observations revealed that at low strains austenite was deformed by planar slip of dissociated dislocations and mechanical twinning (Figs. 9÷11). In the range of medium strains micro-shear bands started to appear within the austenite bands (Figs. 12a,b). It should be noted, that the mechanical twinning occurred in the austenitic γ-phase at the early stages of deformation resulting in formation of the alloy type texture already after 30% of reduction.

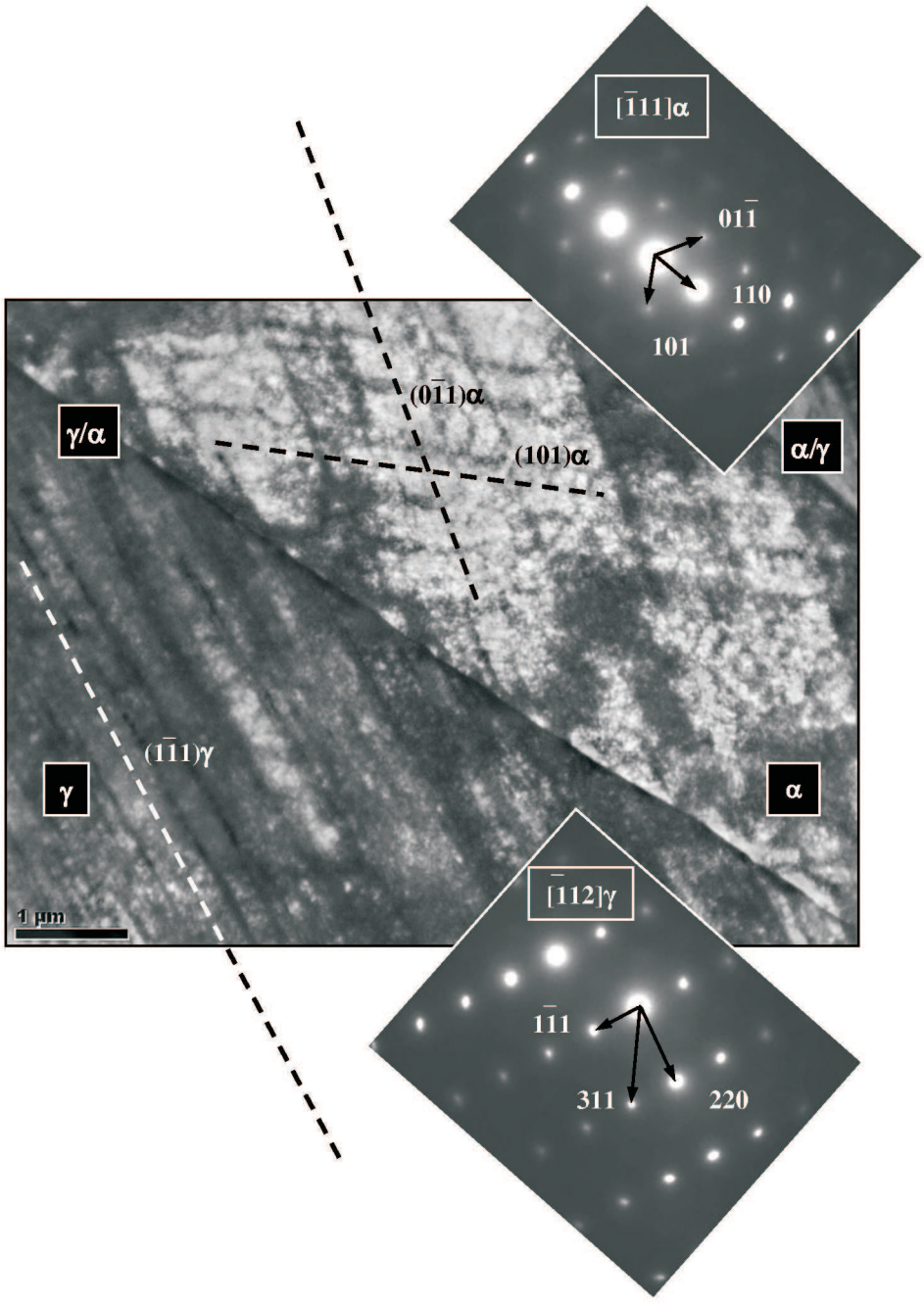

Fig. 9. Microstructures in austenite and ferrite bands after 30% reduction showing slip systems symmetrical to the (α/γ) phase interface

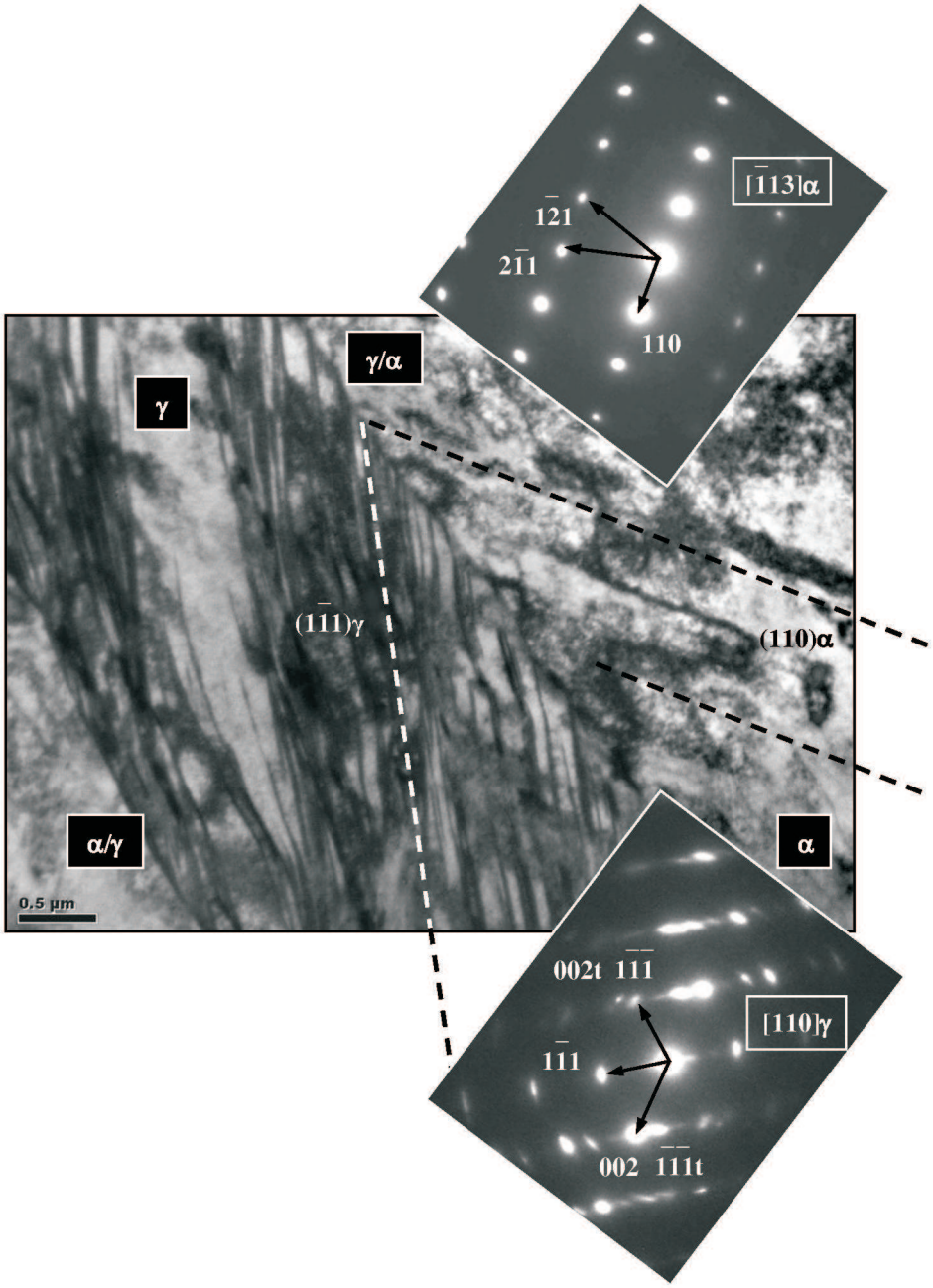

Fig. 10. Microstructures in ferrite and austenite bands after 30% reduction showing slip and twin systems operating adjacent to the (α/γ) phase interface

Depending on a local orientation one or two sets of deformation twins were observed within the single and elongated grains of austenite (Figs. 10, 11). The appearance of mechanical twinning as a major deformation mechanism starting from relatively small strains was apparently the effect of low SFE value [3,4]. With increasing reduction another structural effect was observed, that is the micro-shear bands formed on a background of mechanical twins (Figs. 12a,b) [15]. Microstructure observations indicate that at medium strains their extent is confined only to the austenite areas. The wavy or corrugated shape of the austenite bands frequently observed at higher strains was the result of local shearing of the (α/γ) interfaces by micro-shear bands running through the twinned structure (Fig. 13). Another consequence of low SFE value was the stability of the austenitic γ-phase upon cold-rolling of examined duplex steel. X-ray measurements and microstructure examination did not reveal any contribution of deformation-induced ($\gamma \rightarrow \alpha$) phase transformation. A number of works indicates at the austenite stabilizing role of nitrogen in duplex type steels [3, 4, 14].

In the ferritic α-phase the {001}<110> rotated cubic orientation was the strongest texture compo-

nent during the thermo-mechanical treatment and upon the subsequent cold-rolling. For that orientation there are four equally stressed slip systems {110}<111> with the value of relative shear stresses m=0,816. Even though the four {110} slip planes are identically inclined to the rolling direction RD (Fig. 8a) not all of these slip systems are expected to operate simultaneously.

Microstructure of deformed ferrite typical for lower rolling reductions is shown in Figures 9 and 10, with the bands of increased dislocation density (dense dislocation walls) aligned parallel to the two sets of slip planes symmetrical with respect to the (α/γ) interface. Worthy of notice is a fact that the operation of symmetrical slip (or twin) systems at both sides of the phase interface, with the same or at least approximate values of the relative shear stresses ($m = \tau/\sigma$), should result in plastically compatible deformation of the bands of both phases [16]. With increasing rolling deformation narrow microbands

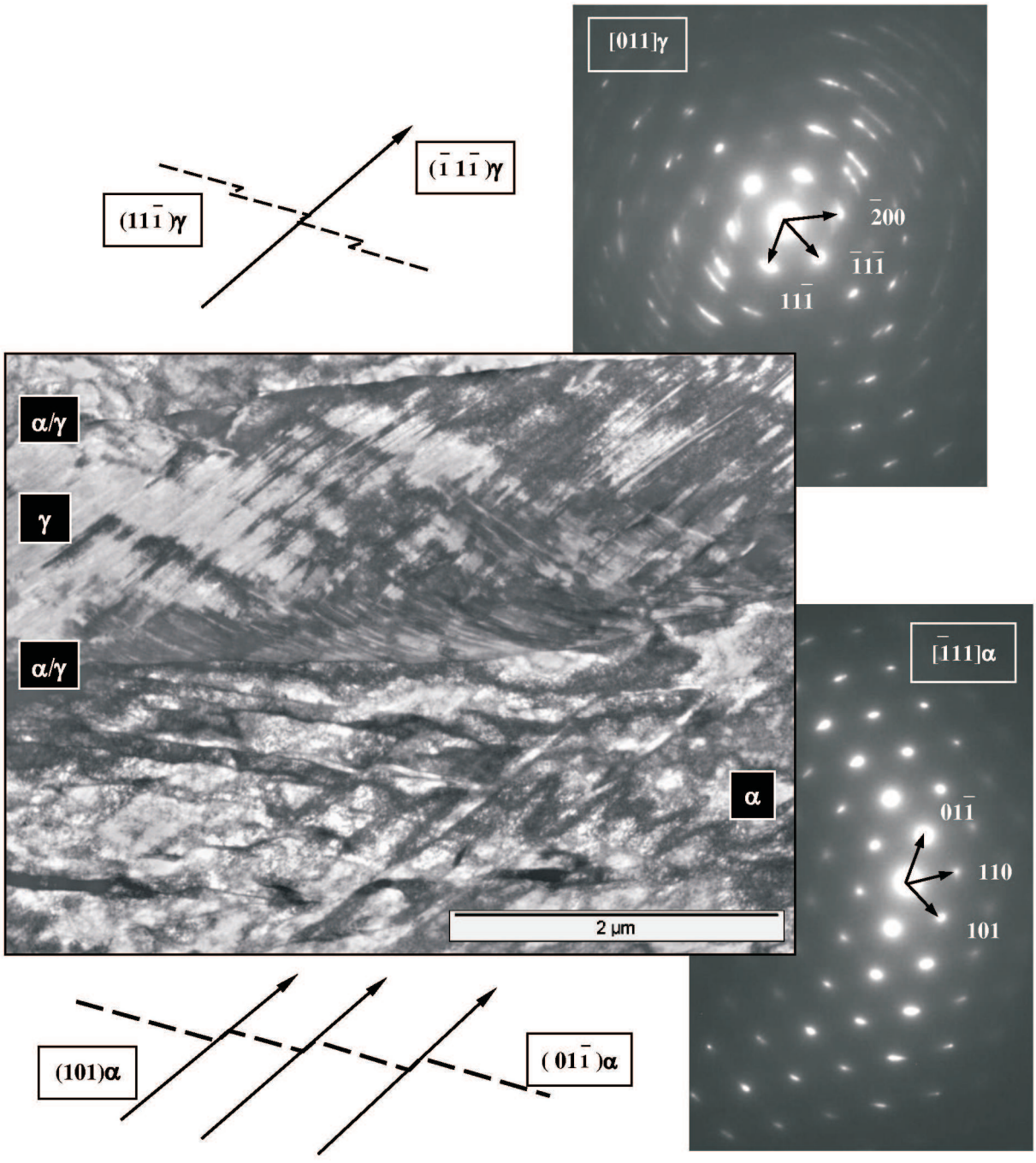

Fig. 11. Microstructure after 50% reduction showing intersecting microbands on a background of high dislocation density in ferrite and mechanical twins within a band of austenite

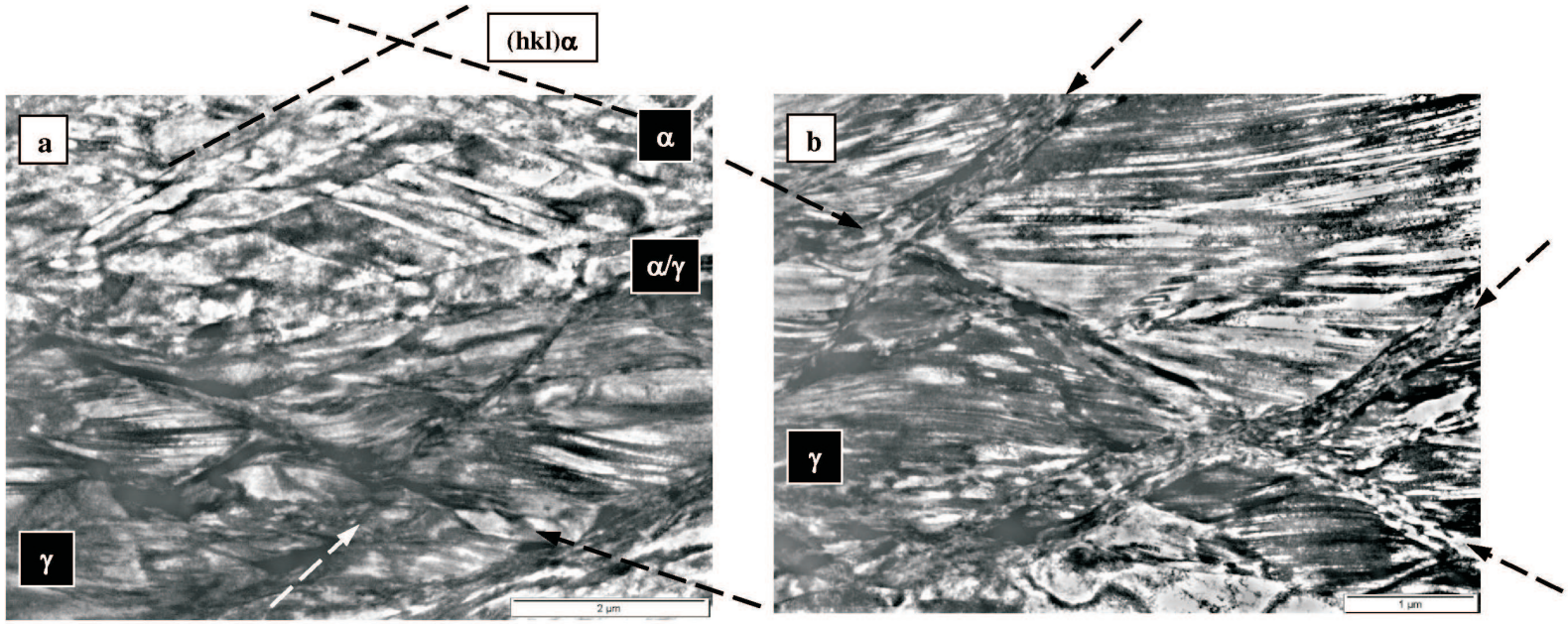

Fig. 12. Two sets of micro-bands in ferrite and micro-shear bands in austenite symmetrical with respect to the (α/γ) interface after 50% reduction (a), formation of shear bands on a background of twined structure in austenite after 70% reduction (b)

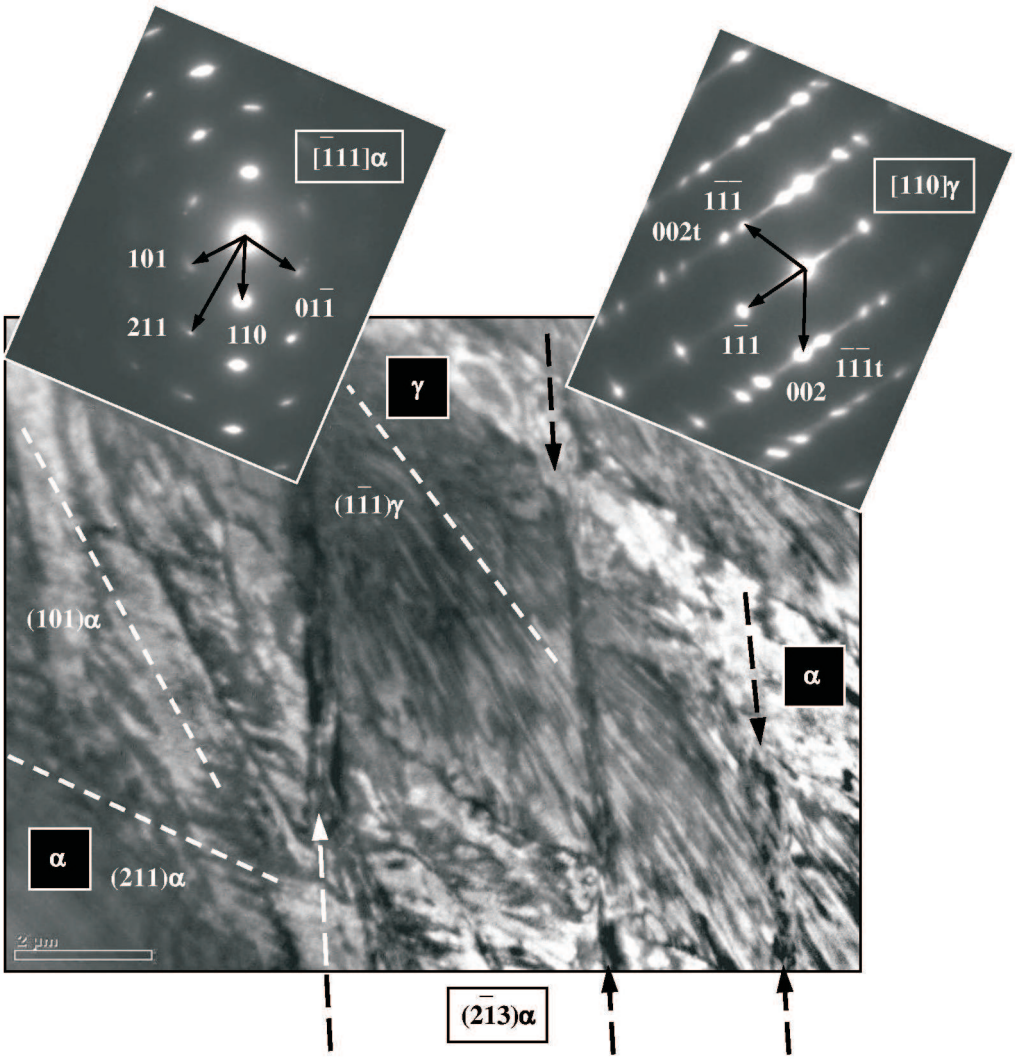

Fig. 13. Micro-shear bands crossing twined structure in austenite and the corrugated shape of the (α/γ) interface resulting from local shear

appeared within the ferrite structure against a background of areas with high dislocation density (Fig. 11, 12b) [15]. These microbands were not necessarily parallel to {110} planes and exhibited typical offsets due to the mutual intersections (Fig.12b). Differences in their direction might result from slip in higher index crystallographic planes. It should be noted that other potential slip systems from the [1$\bar{1}$1] and [$\bar{1}$11] zone axes had also very high relative shear stresses (Fig. 8b). These were two {112}<111> slip systems (m=0.943) and four {123}<111> systems (m=0.926). Despite a higher lattice resistance for a dislocation slip in these planes very high values of the relative shear stresses could result in local slip activation in some of these systems. This effect was observed especially at higher strains, when micro-shear bands formed on the background of twined structure in austenite grains impinged the (α/γ) interfaces resulting in strain localization within the ferrite areas (Fig. 13). Burgers vectors of slip dislocations in the bcc α-phase and the fcc γ-phase are different ($\bar{b}_\alpha$ = a/2<111> and $\bar{b}_\gamma$ = a/2<110>) that is why only slip transfer may occur across the (α/γ) interfaces [16]. Interphase boundaries are apparently strong barriers also for the co-ordinate dislocation motion. It seems that in the case of strong refinement of a band-like two-phase structure, with the band thickness reduced to less than few micrometers, the shear transfer proceeds across the phase interfaces at higher strains (Fig. 13).

4. Concluding remarks

The present research concerned the texture formation and the evolution of ferrite and austenite microstructures in cold-rolled sheets of super-duplex stainless steel UR52N+ (UNS S32520). After the preliminary thermo-mechanical treatment, comprising hot-rolling and solution annealing, the steel

plate was subjected to cold-rolling within a wide range of reductions parallel to the direction of hot-deformation ($RD_C||RD_H$).

The specific band-like morphology of both phases formed upon processing seems to be an important factor affecting the deformation behavior and the formation of ferrite and austenite rolling textures. Deformation mechanisms in both constituent phases of examined super-duplex steel were essentially the same as in single phase steels and the structural effects resulting from their operation were limited to the areas of respective phases. Microstructure development in the ferrite and austenite bands resulted first of all from; crystallographic structure, chemical composition, stacking fault energy and orientation distribution, and only to some extent from phase interaction.

The operation of deformation systems with approximate values of relative shear stresses and symmetrical with respect to RD should result in plastically compatible deformation of ferrite and austenite bands. The micro bands in ferrite and the micro-shear bands in austenite, which reflect the co-ordinate dislocation motion, were also symmetrical in relation to the phase interfaces. These structural effects appeared at medium strains and were confined to the regions of both respective phases. The (α/γ) interfaces laying mostly parallel to the sheet plane seem to be strong barriers even for the co-ordinate dislocation motion throughout two-phase structure. In dependency of local stress state a shear transfer across the phase interfaces was frequently observed at higher strains, resulting in corrugated shape of the (α/γ) interfaces. It seems that in the case of two-phase banded structure the formation of shear bands typical for one-phase steels is strongly hindered and the occurrence of shear banding may be limited only to one-phase areas.

The texture analysis indicates at the stability of rolling textures in both constituent γ- and α- phases over a wide range of reductions, up to about 85% of deformation. Comparison of the rolling texture formation after solution annealing at the temperatures 1150°C and 1050°C, that is for different phase fractions of ferrite and austenite (V_V^F ~60%, V_V^A ~40% and $V_V^F = V_V^A$ ~50% respectively), did not reveal significant qualitative differences in a texture character.

The austenitic γ-phase showed tendency to develop the rolling textures similar to those in one-phase austenitic steels with the major texture component close to the alloy type orientation. The {110}<112> orientation was stable and dominant texture component from about 30% of reduction up to high strains. The addition of nitrogen (0.26%N) and its concentration mainly within the γ-phase considerably decreased stacking fault energy and as a result the austenite rolling textures in the examined super-duplex steel resembled those in low SFE alloys. Small value of stacking fault energy determined the deformation behavior of austenite, which was deformed by twinning starting from relatively low strains. Another consequence of low SFE value was the stability of the austenitic γ-phase upon cold-rolling. X-ray measurements and microstructure examination gave no evidence for deformation induced $(\gamma \rightarrow \alpha)$ phase transformation.

The rolling textures of the α-phase differed from those in single phase ferritic steels. The major component of the ferrite starting texture, i.e. the {001}<110> rotated cubic orientation, was stable up to high deformations. Similarly the character of texture spread remained essentially the same over the whole deformation range with only slight changes concerning the minor orientations from the limited α_1- and ε-fibers, that is components of weaker intensities. Very characteristic feature of texture formation in the ferritic α-phase and the most striking difference compared to one-phase steels was the absence of the γ-fiber {111}<uvw> within the ferrite texture of the examined super-duplex steel.

Acknowledgements

The authors wish to thank professors W. Ratuszek and J. Morgiel for discussions and invaluable help. The work was financially supported by the Polish Committee for Scientific Research (KBN) under the contract No. 10.10.110.720.

REFERENCES

[1] G. Fargas, N. Akdut, M. Anglada, A. Mateo, Microstructural Evolution during Industrial Rolling of a Duplex Stainless Steel, ISIJ International, **48**, 1596-1602 (2008).

[2] C. Herrera, D. Ponge, D. Raabe, Microstructure and Texture of Hot-rolled Duplex Stainless Steel, Proc. 3rd Int. Conf. on Thermo-Mechanical Processing of Steels, Padua, Italy (2008).

[3] N. Akdut, J. Foct, Microstructure and Deformation Behavior of High Nitrogen Duplex Stainless Steel, ISIJ International., **36**, 883-892 (1996).

[4] J. Keichel, J. Foct, G. Gottstein, Deformation and Annealing Behaviour of Nitrogen Alloyed Duplex Stainless Steels. Part I: Rolling, ISIJ International, **43**, 1781-1787 (2003).

[5] N. Akdut, J. Foct, G. Gottstein, Cold Rolling Texture Development of (α/γ) Duplex Stainless Steel, Steel Research, **67**, 450-455 (1996).

[6] J. Ryś, W. Ratuszek, M. Witkowska, Rolling Texture Differences in Duplex Steels with Strong and Random Initial Textures, Solid State Phenomena **130**, 57-62 (2007).

[7] J. Ryś, W. Ratuszek, Rolling Texture Formation in Super-Duplex Stainless Steel, Solid State Phenomena **163**, 145-150 (2010).

[8] W.B. Hutchinson, K. Ushioda, G. Runnsjö, Anisotropy of Tensile Behaviour in a Duplex Stainless Steel Sheet, Mater. Science and Techn., **1**, 728-731 (1985).

[9] D. Raabe, K. Lücke, Textures of Ferritic Stainless Steels, Mater. Science and Techn., **9**, 302-312 (1993).

[10] D. Raabe, Texture and Microstructure Evolution during Cold Rolling of a Strip Cast and of a Hot Rolled Austenitic Stainless Steel, Acta Materialia, **45**, 1137-1151 (1997).

[11] J.-O. Nilsson, Super Duplex Stainless Steels, Materials Science & Technology, **8**, 685-700 (1992).

[12] Tselikov, Stress and Strain in Metal Rolling, Mir Publishers, Moscow (1967).

[13] J. Ryś, M. Witkowska, P. Matusiewicz, The Effect of Solution Treatment and Nitrogen Addition on Phase Composition of Duplex Steels, Archives of Metallurgy and Materials **53**, 229-236 (2008).

[14] W. Reick, M. Pohl, A.F. Padilha, Determination of Stacking Fault Energy of Austenite in a Duplex Stainless Steel, Steel Research, **67**, 253-256 (1996).

[15] M. Blicharski, Structure of Deformed Ferrite-Austenite Stainless Steel, Metal Science, **18**, 92-98 (1984).

[16] J. Ryś, Compatibility Effects at Phase Interfaces in Duplex Steel (α/γ) Bicrystals, Journal of Mater. Process. and Techn., **64**, 343-352 (1997).

Received: 10 July 2010.